JOINT CONFERENCE PROCEEDINGS
9th International Conference on Urban Earthquake Engineering/ 4th Asia Conference on Earthquake Engineering
March 6-8, 2012, Tokyo Institute of Technology, Tokyo, Japan

PREDICTING NONLINEAR RESPONSE OF AN RC BRIDGE PIER SUBJECT TO SHAKE TABLE MOTIONS

Zhe Qu[1)]

1) Postdoctoral research fellow, Center for Urban Earthquake Engineering, Tokyo Institute of Technology, Japan
m.quzhe@gmail.com

Abstract: The numerical model, which was used to predict the dynamic response of the reinforced concrete bridge pier in the blind prediction contest held by PEER and NEES in 2010, is described in this paper. The results of this model was rewarded the first place in the researcher category in the contest. The model succeeded in predicting some of the responses, such as the maximum deformation and shear force, while failed in predicting some others, including the residual deformation and the axial force. After the contest, a preliminary parametric study was carried out to see the influence of each parameter in the model. Among many others, it was found that the initial damping ratio and the elastic modulus of the steel rebars were the most influential parameters, whose values were, however, selected based more on empirical judgment than on any rigorous theory.

1. INTRODUCTION

A complicated analysis model does not necessarily ensure better results of prediction than a simple one. An extraordinary example is the win of Professor Kolleger from the Vienna University of Technology in the reinforced concrete slab shear prediction competition held by the ETH in Zurich in 2005. It was reported that his "predicted deformation capacity closely approximated the observed response of all specimens containing transverse reinforcement" (Jaeger, 2006). It is worth noting that his prediction, it was said, was based solely on hand calculation.

The author of this paper participated in the blind prediction contest held by PEER and NEES in 2010 to predict the dynamic response of a full-scale reinforced concrete (RC) bridge pier subjected to a series of shake table motions at UCSD, and unexpectedly won the first place in the researcher category. The numerical model used in this analysis and its results are reported in this paper. The results of a preliminary parameter study are also included at the end of this paper to identify what has been done right to obtain the good prediction. It should be pointed out that the successful prediction was by no means the consequence of the superiority of the author's numerical model over those of the other participants in the same category. Instead, it is no more than an educated guess which is based on a relatively simple model and experience of numerical modeling of RC members.

The specimen, as depicted in Figure 1, is a cantilever circular RC column resting on a rectangular RC foundation and supporting on its top a lumped mass of approximately 250 ton. The foundation was fixed to the shake table through prestressing steel rods. The top mass consisted of five concrete blocks tied together by prestressing steel rods. The seismic excitation was exerted in a single direction, as indicated in Figure 1 by an arrow.

The column is reinforced with 18 #11 deformed steel bars arranged along the perimeter of the cross section and #5 double circular hoops, 3'8" in diameter, at a spacing of 6 inches along the height of the column (Figure 2). There is 2 inches clearance from the hoops to the concrete surface, indicating 84.6mm distance from the centroid of each longitudinal bar to the concrete surface. The yield strength of the #11 rebar provided by the contest committee is 518 MPa. The concrete compressive strength tested at different ages is listed in Table 1.

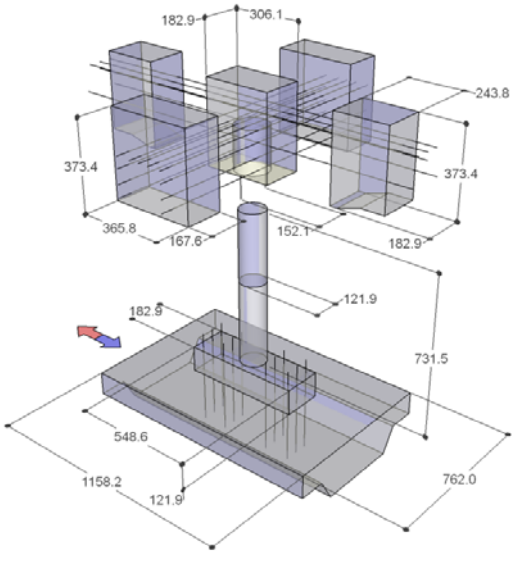

Figure 1 Dimensions of specimen (unit: cm)

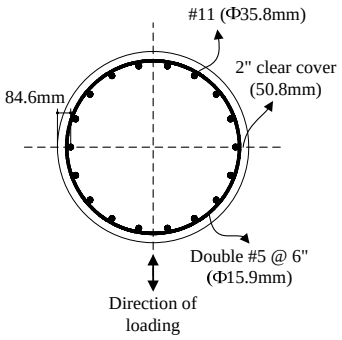

Figure 2 Reinforcement of specimen

Table 1 Test concrete compressive strength

Date tested	Age (days)	f_{c0} (MPa)
2010/8/30	21	36.96
2010/9/20 (1st day of shaking)	42	40.89
2010/9/21 (2nd day of shaking)	43	41.99

2. NUMERICAL MODEL

A finite element model consisting of ten 2-dimensional linear beam elements (type B21) and a point mass element was built in ABAQUS/Standard 6.8 for the specimen (Figure 3). The column was fixed at its base and the concrete foundation was not explicitly modeled. The length of the beam element at the bottom, which was expected to concentrate most the plasticity of the column and thus dominate the nonlinear response of the column during shaking, was selected to be equal the diameter of the column, i.e., 1219mm.

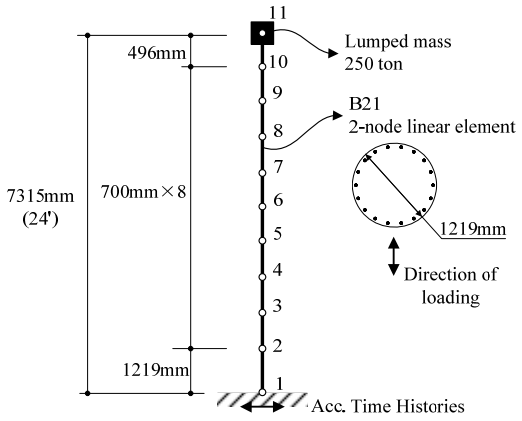

Figure 3 Finite element model of specimen

Additional integration points, denoted as steel fibers hereafter, were inserted into the column cross section, each of which represented a longitudinal rebar. Along the loading direction, 9 integration points, or concrete fibers, were evenly placed for the concrete part of the section.

User-defined uniaxial hysteresis of the steel and the concrete fibers was adopted. It is part of a more general collection of uniaxial hysteretic models of commonly-used constructional materials, namely PQ-Fiber, for the simulation of seismic response of building structures, which was developed by Qu (2007) and his colleagues. The hysteretic model used for the blind analysis contest is labeled in PQ-Fiber as STEEL02 for the steel fiber and CONCRETE02 for the concrete model.

The hysteretic model for the steel fiber is basically the peak oriented model proposed by Clough (1966) with two modifications. Firstly, the material reloads with its unloading stiffness up to 0.2 times the maximum stress ever achieved in the reloading direction before it orients to the peak point (Figure 4). Secondly, a strength deterioration model based on effectual hysteretic energy dissipation proposed by Qu (2010) is incorporated.

The hysteretic model for the concrete fiber is the same as the model of Concrete02 in OpenSEES (McKenna, 1997). The deterioration of the stiffness in both tension and compression and that of the tensile strength are taken into account (Figure 5).

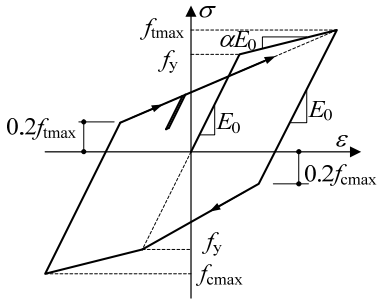

Figure 4 Stress-strain relationship of steel fiber

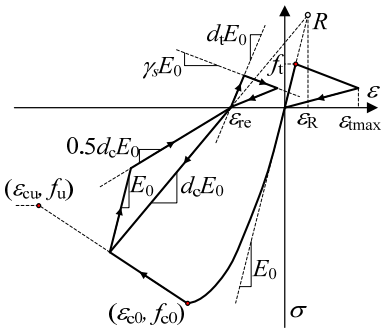

Figure 5 Stress-strain relationship of concrete fiber

Table 2 Parameters of material models

	Parameter	Value
Concrete	Compressive strength f_{c0}	40.89 MPa
	Peak strain ε_{c0}	0.0028
	Residual strength f_u	0.8 f_{c0}
	Ultimate strain ε_{cu}	0.0038
	Compressive damage factor d_{cu}	0.5
	Tensile strength f_t	1.0 MPa
	Tensile softening factor γ_s	0.1
Rebar	Elastic modulus E_s	104 GPa
	Yield strength f_y	518 MPa
	Post-yield stiffness ratio α	0.001
	Damage factor	52

The values of the parameters that define the above material models, which were adopted for the blind analysis

contest, are listed in Table 2. The concrete compressive strength, f_{c0}, and the steel yield strength, f_y, were taken as their test values published by the contest committee, while the others were chosen empirically (e.g., f_u, ε_{cu}, d_{cu}, f_t, γ_s and α) or based on some empirical modification of the test values (e.g., the concrete peak strain, ε_{c0} and the steel elastic modulus, E_s).

The stress-strain curve obtained by concrete cylinder compressive test at 21-day age was provided, from which both the compressive strength f_{c0} and the peak strain ε_{c0} could be determined. In the analysis, f_{c0} was chosen to be the 42-day strength of 40.89 MPa, which was obtained on the first day of shaking, and the peak strain, ε_{c0}, was assumed to be the same as that obtained at 21-day age (Figure 6).

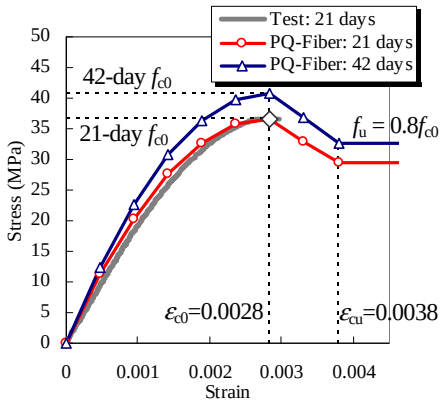

Figure 6 Skeleton curve of concrete fiber

The measured elastic modulus of steel was 208 GPa. In the analysis, however, it was empirically taken as half the measured value (Figure 7). It was mainly an effort to reduce the initial stiffness of RC members, which, to the author's experience, is frequently over-estimated with the measured elastic modulus of steel. The effect of this modification will be shown later in this paper.

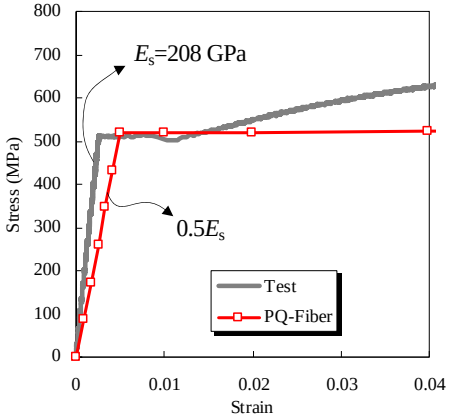

Figure 7 Skeleton curve of steel fiber

The hoop in the column was not explicitly modeled. In addition, neither the shear failure of the column nor the anchorage failure of the longitudinal rebars was taken into account.

Mass proportional damping was used and the damping ratio corresponding to the first mode, which is 0.609 second, was assumed to be 2%.

3. INPUT MOTIONS

The recorded table motions were first processed by a Butterworth band pass filter before being used as the input for the analysis. The frequency band was arbitrarily decided to be 0.1 Hz ~ 5 Hz. The peak values of the shake table motions were considerably changed by the filtering, as can be seen in Table 3, while the response spectra remained almost unchanged within the useful frequency range (Figure 8). The filtering was believed to have little effect on the prediction results. White noise excitations between these major runs were not simulated.

Table 3 Earthquake motions simulated by shake table

Test	Original NGA File	Recorded		Filtered	
		PGA (g)	PGV (cm/s)	PGA (g)	PGV (cm/s)
Run 1	AGW090.at2	0.195	17.59	0.133	14.55
Run 2	CLS090.at2	0.411	38.50	0.366	38.99
Run 3	LGP000.at2	0.515	85.39	0.457	80.95
Run 4	CLS090.at2	0.445	40.11	0.397	42.10
Run 5	TAK000.at2	0.540	94.01	0.477	98.53
Run 6	LGP000.at2	0.496	98.64	0.441	80.56

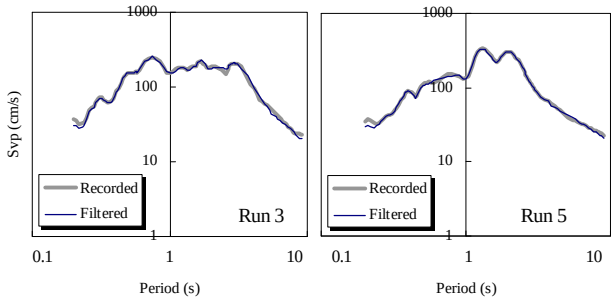

Figure 8 Pseudo velocity spectra of shake table motions (5% damping)

4. ANALYSIS RESULTS

The analysis was conducted in series for the 6 runs of the test so that the damage of the column, generally in terms of strength and stiffness deterioration, during a previous run would go into the following run. While the strength deterioration in this test seemed to be insignificant, the deterioration of the reloading stiffness and its effect on the following runs can be observed in Figure 9, which depicts the predicted moment-curvature relationship at the column bottom for each run. A static pushover curve produced by Response 2000 (Bentz et al, 2001) is also plotted in those graphs. According to the analysis, the column remains essentially elastic during the first two runs, which have peak ground velocities (PGVs) of 14.55 cm/s and 38.99 cm/s, and goes deep into the plastic range in Run 3 with PGV of 80.95

cm/s. The ratio of maximum to yield curvature reaches greater than 4 in this run. After Run 4 whose intensity is relatively low, Run 5, the well-known Takatori motion recorded in 1995 Kobe earthquake, brings the column to yield in not only the previously yielded direction in Run 3, but also the other direction. The last run also performs a strong motion and it is performed when the column has been extensively damaged. However, the maximum deformation of the column does not much exceed those in the previous runs.

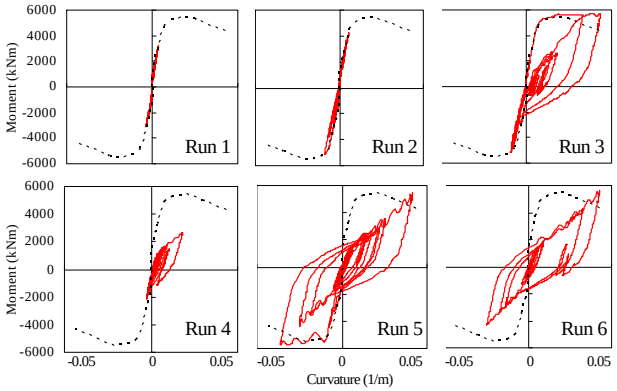

Figure 9 Predicted bottom moment-curvature relationship

By comparing the predicted results with the measured ones, it can be found that the above numerical model succeeded in predicting the maximum drift, the maximum base shear and the maximum base moment for every run of the test (Figure 10(a), (c) and (d), where the horizontal axis indicates the number of run). The relative errors of the predicted results corresponding to the measured ones were generally below or around 20% for these quantities. These well-predicted quantities accounts for more than half the answers required by the blind analysis contest.

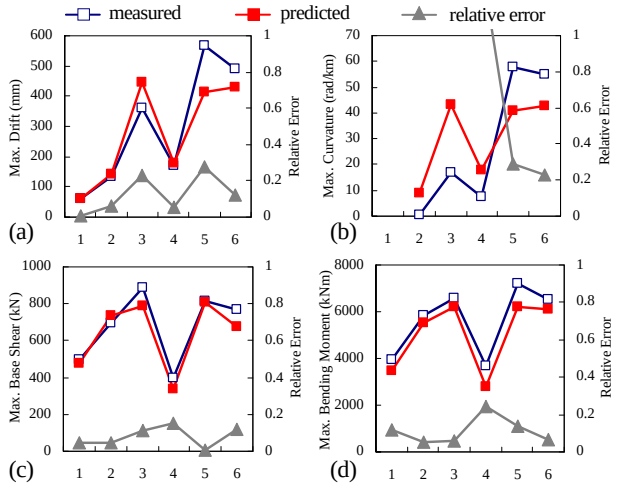

Figure 10 Predicted and measured results: (a) maximum drift; (b) maximum curvature at bottom; (c) maximum base shear and (d) maximum moment at bottom.

It is, however, obvious that the model failed to yield good estimate of some other responses, such as the curvature at the column bottom (Figure 10(b)). The curvature was much over-estimated for Run 2, 3, and 4, while was a little under-estimated for Run 5 and 6. While the slight under-estimation of the maximum curvature for Run 5 and 6 corresponds well with that of the maximum top drift for the two runs, the over-estimation for Run 2, 3 and 4 can not be readily explained.

The bottom curvature was averaged within different ranges along the column between in the test and in the analysis. It was taken as the curvature of the bottom element in the analysis, whose length was 1219mm, much greater than the 200mm length within which the averaged curvature was measured in the test. However, this difference was much more likely to contribute to some under-, rather than over-estimation.

With some simple assumption of the curvature distribution along the height of the column, for example, those shown in Figure 11, the bottom curvature, ϕ, and the top drift, Δ, can be readily related by simple equations, e.g., Equation 1.

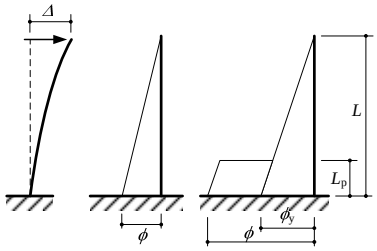

Figure 11 Curvature distribution

$$\Delta = \begin{cases} \phi L^2/3, & \phi \le \phi_y \\ \phi_y L^2/3 + (\phi - \phi_y)\cdot L_p (L - L_p/2), & \phi > \phi_y \end{cases} \qquad (1)$$

where L is the total height of the column; L_p is the assumed length for the plastic hinge and ϕ_y is the yield curvature, which is about 0.01/m for the investigated column

The relationship of the predicted Δ and ϕ is plotted in Figure 12, together with the measured maximum values. Assuming L_p equals the length of the bottom element, i.e., 1219mm, the relationship in Equation 1 would match well the analysis result. In addition, the assumed curvature distribution in Figure 11 and the assumed plastic hinge length L_p can also well explain the measured data of Run 5 and 6. It is, however, quite otherwise for Run 2 and 3.

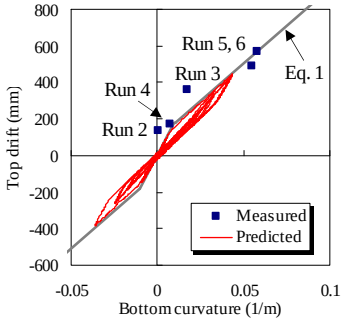

Figure 12 Lateral drift versus bottom curvature relationship

The numerical model also failed to yield satisfactory estimate of some other important response quantities, e.g., the residual deformation and the axial force of the column. The predicted residual drift was much smaller than the observed ones for Run 3 through Run 6. Furthermore, the residual drift in Run 3 disappeared in Run 5 in the analysis. It was not the case in the test (Figure 13(a)).

For the maximum axial compressive force, no significant variation between different runs was observed in the test. In the analysis, however, the maximum axial compressive force in a plastic run, e.g., Run 3, was much greater than that in an essentially elastic run, e.g., Run 1 (Figure 13(b)). For a flexural RC member, the neutral axis of cracked sections moves towards the compressive side, leading to extension of the member's center line. This explains the significant variation of axial force in the analysis, which is directly associated with that of the vertical acceleration.

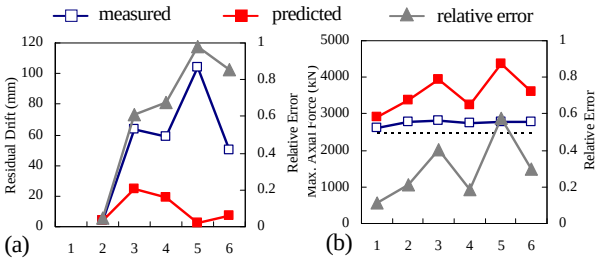

Figure 13 Predicted and test results: (a) residual deformation and (b) maximum axial compressive force

The thus-produced vertical acceleration seems to depend highly on concrete material model used in the analysis. The vertical acceleration responses given by two inherent concrete models in ABAQUS, namely the concrete damaged plasticity model and the smeared crack model, are compared in Figure 14 with that by Concrete02 in PQ-Fiber. Identical model is adopted for the steel fiber in all the three analysis. Very different results can be observed.

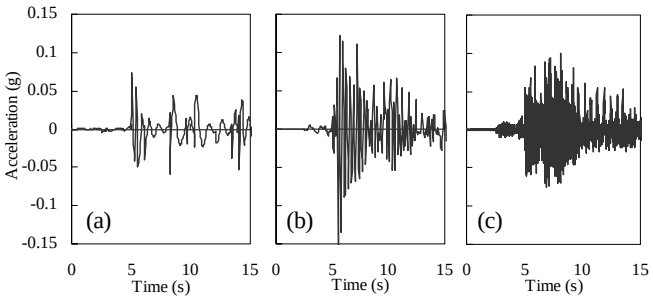

Figure 14 Vertical acceleration at column top predicted by models with (a) concrete damaged plasticity model; (b) concrete smeared crack model and (c) Concrete02 in PQ-Fiber

5. PARAMETRIC STUDY

In order to identify the sensitive parameters in the current model, a parametric study is conducted after the contest. At this stage, the predicted results by the above-mentioned models (referred to as the original model hereafter) are taken as the reference for comparison. The quantities listed in Table 4 are compared between the original model and the altered models.

Many modeling parameters are investigated and are identified as not so much influential when they are taken within their respective reasonable ranges. These include: (1) size of the bottom element; (2) steel hardening stiffness ratio; (3) steel damage factor; (4) concrete elastic modulus and (5) concrete tensile behavior.

Table 4 Quantities compared in parametric study

Label	Physical quantity
δ_{max}	Maximum lateral drift at the top
δ_{amp}	Absolute value of the maximum positive plus that of the maximum negative lateral drift
A_{max}	Maximum total acceleration at the top
F_{max}	Maximum base shear
M_{max}	Maximum moment at the bottom
N_{max}	Maximum axial force at the bottom
ε_{Tmax}	Maximum tensile strain at the bottom
ε_{Cmax}	Maximum compressive strain at the bottom

It was, however, identified that both the global and the local responses or only some local responses are quite sensitive to some other parameters, including (1) the initial damping ratio, (2) steel elastic modulus and (3) concrete ultimate strength.

5.1 Initial damping ratio

The initial damping ratio is typically assumed in the range of 2% ~5% for dynamic analysis of building structures in the US (FEMA P695, 2009). An initial damping ratio of 2~3% is generally used in the design practice of RC building in Japan following the reported measurement conducted by AIJ (2000). This coincides with the values recommended by Newmark et al (1982) for well-reinforced concrete structures at their working stress level. It is, however, frequently assumed to be 5% in linear and nonlinear dynamic analysis of RC structures in China, as is encouraged by the seismic design code (GB50011, 2010).

In nonlinear analysis, the assumed initial damping should be less than that in a linear analysis because the energy dissipation due to the nonlinearity of materials should be taken into account in the nonlinear material model. In addition, the assumed initial damping for the analysis of a single cantilever column should be less than that of a real building structure because the portion of energy dissipation arising from nonstructural components is almost zero in the former case. It was based on these considerations that 2% initial damping, which seems to be the lower bound for the seismic analysis of RC structures, was adopted in the original model.

The initial damping ratio has considerable influence on the prediction of both the local and the global response of the column, especially when the column remains essential elastic, e.g., in Run 1 (Figure 15). If the damping ratio is

increased from 2% to 5%, the maximum drift, as well as the maximum base shear and moment, would be reduced by about 20%~30% during Run 1 (Figure 16(a)). Because of the yielding of the column, the maximum force responses become independent on the initial damping ratio while the maximum drift is still reduced by more than 20% for Run 3 (Figure 16(b)). The influence of the initial damping seems to vanish in Run 5, during which the hysteretic energy dissipation takes a much greater part of the total energy dissipation than in the precious runs (Figure 16(c)).

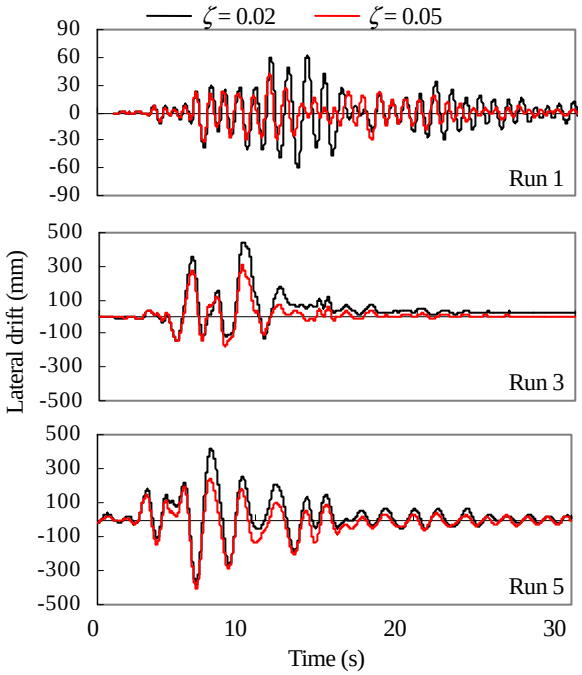

Figure 15 Time histories of top drift predicted by models with different initial damping ratio

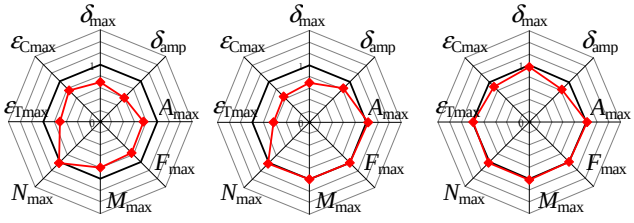

Figure 16 Ratios of maximum responses predicted with 5% to those with 2% initial damping ratio

5.2 Steel elastic modulus

The use of $0.5E_s$ instead of the measured value, E_s, as the elastic modulus of the steel fibers in the original model (Figure 17) was solely an empirical judgment in order to reduce the initial stiffness of the RC column. The change in stiffness is accompanied by the shift of the vibration period of the column, which is likely to greatly affect the predicted maximum responses of the column depending on the characteristics of the response spectrum of the input motions. It is found after the contest that the use of this reduced steel elastic modulus may greatly affect the prediction results of both the force and the deformation responses when the column remains essentially elastic (Figure 18(a)) and the deformation response after the column yields (Figure 18(b) and (c)). The moment-curvature curves for Run 1, 3 and 5 predicted by models using different steel elastic moduli are compared in Figure 19. The change in stiffness is obvious.

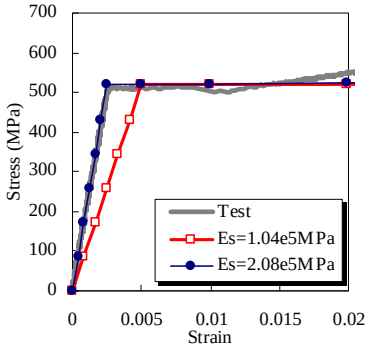

Figure 17 Steel fiber skeleton curves with different elastic moduli

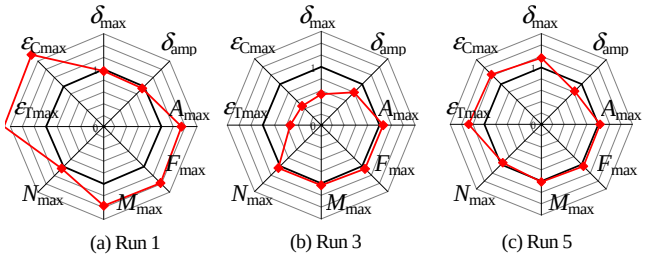

Figure 18 Ratios of maximum responses predicted with measured E_s to those with $0.5E_s$

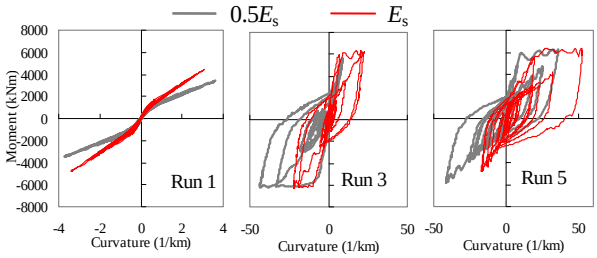

Figure 19 Bottom moment-curvature relationship predicted with different steel elastic moduli

5.3 Concrete post peak behavior

In the original model, it was assumed that the concrete fiber is able to keep 80% of its strength after the peak strain is exceeded. This is beneficial for the convergence of the numerical computation, but may over-estimate the capacity of the concrete. By comparing the results obtained by $f_u = 0.8f_{c0}$ and $f_u = 0.2f_{c0}$, as shown in Figure 20, it is found that the concrete post peak behavior may greatly influence the maximum compressive strain at the bottom of the column while its influence on the global responses is quite limited (Figure 21 (a) and (c)). From the moment-curvature curves it can be seen that the post-peak stiffness of the column is less when $f_u = 0.2f_{c0}$ is assumed (Figure 22).

It is also observed that for Run 4, the weak run between Run 3 and Run 5, not only the local compressive strain, but

also the maximum force response is considerably reduced if $f_u = 0.2f_{c0}$ is assumed (Figure 21 (b)). It is a consequence of the reduced post peak stiffness of the member, as can be seen in Figure 22.

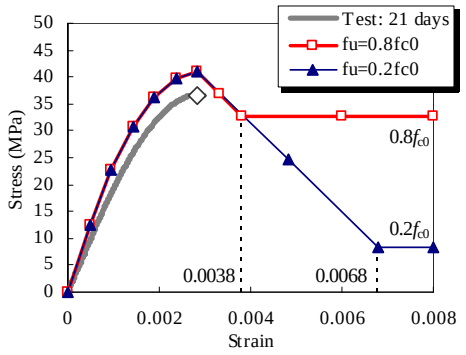

Figure 20 Concrete fiber skeleton curves with different ultimate strength

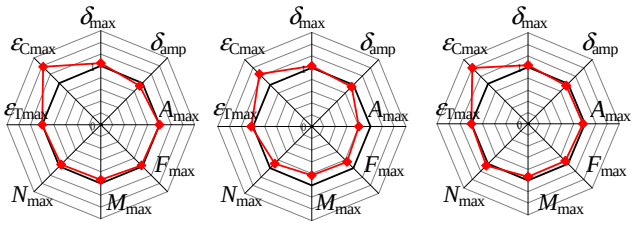

(a) Run 3 (b) Run 4 (c) Run 5

Figure 21 Ratios of maximum responses predicted with $f_u = 0.2f_{c0}$ to those with $f_u = 0.8f_{c0}$

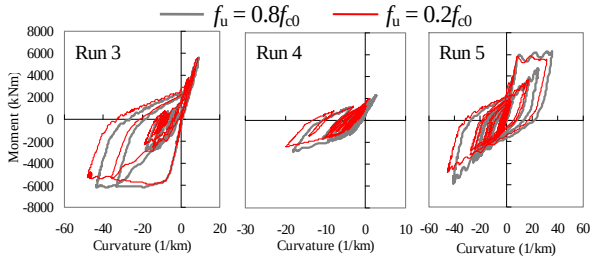

Figure 22 Bottom moment-curvature relationship predicted with different concrete ultimate strength

6. CONCLUDING REMARKS

The numerical model used for the blind prediction contest jointly organized by PEER and NEES in 2010 is described in details. A parametric study is also conducted to identify the influential factors in the numerical model.

The results of the blind prediction and the parametric study after the contest indicate that:

(1) At least the strength of flexural reinforced concrete members can be estimated with confidence;

(2) Other quantities, including the nonlinear maximum drift, can also be well estimated. However, the parametric study reveals that the successful estimation presented in this paper is primarily the consequence of a good guess on the initial damping ratio and an arbitrarily reduced elastic modulus of the steel rebars. The influence of the initial damping ratio may diminish as the member goes deep into the plastic range, while that of the reduced steel stiffness exists in the full range of the member's response.

(3) Residual drift seems more difficult to estimate than the maximum one. There is great space to improve the current numerical model to give better estimate for the residual deformation.

It should be pointed out that any conclusion drawn from a single model for a single analysis may be incomplete. More complete understanding of the advantages and disadvantages of different modeling techniques may be obtained by collecting and comparing the models of all the participants of the blind analysis contest.

References:

AIJ (2000), "Damping in buildings," Architectural Institute of Japan: 189-213.

Bentz, E., Collins, M. P. (2001). "Response 2000 manual," http://www.ecf.utoronto.ca/~bentz/r2k.htm

Clough, R. W. (1966), "Effect of stiffness degradation on earthquake ductility requirements," SESM 66-16, Department of Civil Engineering, University of California, Berkeley

FEMA P695 (2009), "Quantification of building seismic performance factors," Federal Emergency Management Agency: 6-13.

GB50011 (2010), "Code for seismic design of buildings," National Standard of P.R. China.

Jaegar, T. (2006), "Reinforced concrete slab shear prediction competition," *fib*-news, Dec., 2006

McKenna, F. (1997), "Object oriented finite element programming: frameworks for analysis, algorithms and parallel computing," University of California, Berkeley, California, U.S.

Newmark, N. M., Hall, W.J. (1982), "Earthquake spectra and design," Earthquake Engineering Research Institute, Berkeley, Cali.: 54

Qu, Z. (2007), "A collection of user-defined uniaxial hysteretic models for ABAQUS/Standard," http://www.quzhe.net/PQFiber-en.htm

Qu, Z., Ye, L.P. (2010), "Strength deterioration model based on effective hysteretic energy dissipation for RC members under cyclic loading," Proc.7th Intl. Conf. on Urban Earthquake Eng.(7CUEE) & 5th Intl. Conf. on Earthquake Eng.(5ICEE), 2010: 851-856